Combined Effects of Diamines and Carboxylate Bridges on Structural and Magnetic Properties of a Series of Polynuclear Copper(II) Complexes with 1,1-Cyclobutanedicarboxylic Acid

5 AUTHORS, INCLUDING:

Joan Ribas

374 PUBLICATIONS 11,865 CITATIONS

SEE PROFILE

Miguel Maestro

University of A Coruña

173 PUBLICATIONS 3,166 CITATIONS

SEE PROFILE

Inorganic Chemistry

Article

Combined Effects of Diamines and Carboxylate Bridges on Structural and Magnetic Properties of a Series of Polynuclear Copper(II) Complexes with 1,1-Cyclobutanedicarboxylic Acid

Raúl Baldomá,[†] Montserrat Monfort,*,[†] Joan Ribas,[†] Xavier Solans,[‡] and Miguel A. Maestro[§]

Departament de Química Inorgànica, Universitat de Barcelona, Martí i Franqués 1-11, 08028 Barcelona, Spain, Departament de Cristal·lografia i Mineralogia, Universitat de Barcelona, Martí i Franqués s/n, 08028 Barcelona, Spain, and Departamento de Química Fundamental, Universidade da Coruña, 15071 A Coruña, Spain

Six new copper(II) complexes of formula [Cu(μ-cbdca)(H$_2$O)]$_n$ (**1**) (cbdca = cyclobutanedicarboxylate), [Cu$_2$(μ-cbdca)$_2$(μ-bipy)$_2$]$_n$ (**2**) (bipy = 4,4′-bipyridine), [Cu(μ-cbdca)(μ-bpe)]$_n$ (**3**) (bpe = 1,2-bis(4-pyridyl)ethane), [Cu(μ-cbdca)(bpy)]$_2$ (**4**) (bpy = 2,2′-bipyridine), [Cu(terpy)(ClO$_4$)]$_2$(μ-cbdca)·H$_2$O (**5**) (terpy = 2,2′:6′,2′′-terpyridine), and [Cu(cbdca)(phen) (H$_2$O)]·2H$_2$O (**6**) (phen = 1,10-phenanthroline) were obtained and structurally characterized by X-ray crystallography. Complex **1** is a two-dimensional network with a carboxylate bridging ligand in *syn-anti* (equatorial–equatorial) coordination mode. Complexes **2** and **3** are formed by chains through *syn-anti* (equatorial–apical) carboxylate bridges, linked to one another by the corresponding amine giving two-dimensional nets. Complexes **4** and **5** are dinuclear, with the copper ions linked by two oxo (from two different carboxylate) bridging ligands in **4** and with only one carboxylate showing the unusual bis-unidentate mode in complex **5**. Complex **6** is mononuclear, with the carboxylate linked to copper(II) in a chelated form. Intermolecular hydrogen bonds and π–π stacking interactions build an extended two-dimensional network. Magnetic susceptibility measurements of complexes **1**–**5** in the temperature range 2–300 K show the occurrence of weak ferromagnetic coupling for **1** and **4** ($J = 4.76$ and 4.44 cm^{-1}, respectively) and very weak antiferromagnetic coupling for **2**, **3**, and **5** ($J = -0.94$, -0.67, and -1.61 cm^{-1}, respectively). Structural features and magnetic values are compared with those reported for the similar copper(II) malonate and phenylmalonate complexes.

Introduction

There has been considerable and growing interest in inorganic–organic hybrid materials with variable dimensionality and different coordination frameworks. The studies of these inorganic–organic hybrid structures focus on aspects concerning material science and structural chemistry because of their potential applications in catalysis,[1] absorption processes,[2] photochemistry,[3] and magnetism.[4] In the context of molecular magnetism, the study of magneto–structural

correlations aimed at understanding the structural and chemical factors that govern the exchange coupling between paramagnetic centers through multiatomic bridges is of continuous interest.[4b]

Given the above, the structure and physical properties of polynuclear coordination compounds with different carboxylate-type ligands, such as α,ω-dicarboxylate,[5] phthalate,[6] biphenylcarboxylate,[7] etc., have been the subject of recent reports. One of the most widely studied carbox-

(1) Seo, J. S.; Whang, D.; Lee, H.; Jun, S. I.; Oh, J.; Jeon, Y. J.; Kim, K.; *Nature* **2000**, *404*, 982 and references therein.
(2) Kondo, M.; Okubo, T.; Asami, A.; Noro, S.; Yoshimoto, T.; Kitagawa, S.; Ishii, T.; Matsukawa, H.; Seki, K. *Angew. Chem., Int. Ed. Engl.* **1999**, *38*, 140 and referfences therein.
(3) Ogawa, M.; Kuroda, K. *Chem. Rev.* **1995**, *95*, 399 and references therein.
(4) (a) *Molecular Magnetism: from Molecular Assemblies to Devices.* Coronado, E., Delhaes, P., Gatteschi, D., Miller, J. S., Eds.; NATO ASI Series E321; Kluwer: Dordrecht, The Netherlands, 1996. (b) *Magnetism: Molecules to Materials*; Miller, J. S., Drillon, M., Eds.; Wiley: New York, 2000–2005; Vols. 1–5.
(5) (a) Livage, C.; Egger, C.; Férey, G. *Chem. Mater.* **1999**, *11*, 1546. (b) Livage, C.; Egger, C.; Férey, G. *Chem. Mater.* **2001**, *13*, 410. (c) Livage, C.; Egger, C.; Nogués, M.; Férey, G. *Mater. Chem.* **1998**, *8*, 2743.

ylate−copper systems is that involving malonate-bridged copper(II) complexes, due to their versatility when adding new cooperative ligands to build novel systems with different dimensionalities. Indeed, Ruiz-Pérez and co-workers have exhaustively studied the structural and magnetic properties of this kind of compound, demonstrating that malonate is a flexible and fruitful tool for the design of magnetic systems with different dimensionality when an appropriate coligand is used.[8] These authors mainly emphasized structural and magnetic features: from a structural point of view, the coordination of malonate−when acting as a bridging ligand− is currently through the *syn-anti* or *anti-anti* coordination modes.[8,9] From a magnetic point of view the *syn-anti* conformation can give noticeable magnetic coupling, whereas the *anti-anti* conformation always gives almost negligible magnetic coupling. Furthermore, they have found that the parameters governing the magnetic interactions between metal centers are the relative positions of the carboxylate bridge of the malonate with respect to the copper(II) ions: equatorial−equatorial (relatively strong interaction); equatorial−apical (weak interactions); apical−apical (negligible interaction). Within this division, two additional parameters become important: the value of the dihedral angle between the mean basal planes of the interacting copper(II) ions in the equatorial−equatorial exchange pathway and the distortion τ ($\tau = 0$ and 1 for square pyramidal and trigonal bipyramidal copper(II) environments, respectively)[10] in the equatorial−apical one.[11]

These results have been extrapolated to a few other malonate derivatives such as phenylmalonate[9] and benzylmalonate.[12] Indeed, the various coordination modes of the malonate ligand have recently been reviewed.[13]

In light of all these results, the question of whether other conformations of malonate−copper(II) complexes are possible remains open. With this in mind, we began a systematic study with another malonate derivative, the cyclobutanedicarboxylate dianion (hereafter named cbdca). The presence of the cyclobutane ring on the methylene carbon could induce different conformations of the malonate bridging modes due to geometrical constraints. The cbdca ligand has scarcely been used in the synthesis of different complexes with

paramagnetic metal ions,[14] and nonmagnetic studies are performed. However, it has been widely used as a ligand with other nonmagnetic metal ions such as palladium, platinum, and ruthenium for its antitumor activity.[15]

As occurs with malonate and phenylmalonate ligands, the dimensionality of the structures of copper(II)−cbdca complexes will likely be modified in the presence of suitable ligands such as 4,4′-bipyridine (bipy), 1,2-bis(4-pyridyl)-ethane (bpe), 2,2′-bipyridine (bpy), 1,10-phenanthroline (phen), etc. The efficiency of these ligands depends on the extent of their rigidity, and this allows a certain degree of control to be exerted over the steric constraints of the assembly process. In general, the use of bipy and bpe has yielded a wide variety of coordination polymers, some of them featuring unprecedented physical phenomena (porosity, catalysis, molecule absorption, etc.).[16] In this paper, we report the synthesis, crystallographic analysis, and magnetic properties of the first six cyclobutanedicarboxylate copper(II) complexes, starting from the simple copper(II) salt (without any other ligand) and following with five different derivatives by adding specific ligands: bis-monodentate (such as bipy or bpe); bidentate chelated (such as bpy and phen); tridentate (such as terpy). The starting [Cu(H$_2$O)(cbdca)] is a 2D system,[17] which by reaction of different amines gives two novel 2D networks, two different dinuclear complexes, and one mononuclear. When the corresponding structures were compared with those previously described for malonate and phenylmalonate, neither the structures nor the magnetism proved to be identical, thus confirming that the cyclobutane ring added to the malonate framework is not "innocent" with respect to these two features. It can be concluded that, in most cases, it remains difficult to predict the exact structures and composition of the assembly products formed by mixed ligands when subtle variations are introduced into the main skeleton of the ligand (in this case, malonate).

Experimental Section

Synthesis of Compounds. The reagents and solvents used were of commercially available reagent quality, unless otherwise stated.

Caution! Perchlorate salts of metal complexes with organic ligands are potentially explosive. Only a small amount of material should be prepared, and it should be handled with care.

[Cu(μ-cbdca)(H$_2$O)]$_n$ (1). Method A. A solution of H$_2$cbdca (cyclobutanedicarboxylic acid) (0.288 g, 2 mmol) in water (25 cm^3)

(6) Huang, Z. L.; Drillon, M.; Masciocchi, N.; Sironi, A.; Zao, J. T.; Rabu, P.; Panissod, P. *Chem. Mater.* **2000**, *12*, 2805 and references therein.

(7) Pan, L.; Ching, N.; Huang, X.; Li, J. *Inorg. Chem.* **2000**, *39*, 5333. (b) Pan, L.; Finkel, B. S.; Huang, X.; Li, J. *Chem. Commun.* **2001**, 105.

(8) Pasán. J.; Sanchiz, J.; Ruiz-Pérez, C.; Lloret, F.; Julve, M. *Eur. J. Inorg. Chem.* **2004**, 4081 and references therein.

(9) (a) Pasán, J.; Sanchiz, J.; Ruiz-Pérez, C.; Lloret, F.; Julve, M. *New J. Chem.* **2003**, *27*, 1557 and references therein. (b) Cui, G.-H.; Li, J.-R.; Hu, T.-L.; Bu, X.-H. *J. Mol. Struct.* **2005**, *738*, 183 and references therein. (c) Pasán, J.; Sanchiz, J.; Ruiz-Pérez, C.; Lloret, F.; Julve, M. *Inorg. Chem.* **2005**, *44*, 7794 and references therein.

(10) Addison, A. W.; Rao, T. N.; Reedijk, J.; van Rijn, J.; Verschoor, G. C. *J. Chem. Soc., Dalton Trans.* **1984**, 1349.

(11) Pasán, J.; Delgado, F. S.; Rodríguez-Martín, Y.; Hernández-Molina, M.; Ruiz-Pérez, C.; Sanchiz, J.; Lloret, F.; Julve, M. *Polyhedron* **2003**, *2*, 2143.

(12) Castiñeiras, A.; Sicilia-Zafra, A. G.; González-Pérez, J. M.; Choquesillo-Lazarte, D.; Niclós-Gutiérrez, J. *Inorg. Chem.* **2002**, *41*, 6956.

(13) Rodríguez-Martín, Y.; Hernández-Molina, M.; Delgado, F. S.; Pasán, J.; Ruiz-Pérez, C.; Lloret, F.; Julve, M. *CrystEngComm* **2002**, *4*, 522 and references therein.

(14) (a) Pajunen, A.; Pajunen, S. *Acta Crystallogr.* **1979**, 2401−2403. (b) Rzączyńska, Z.; Bartyzel, A.; Głowiak, T. *Polyhedron* **2003**, *22*, 2595.

(15) (a) Barnham, K. J.; Djuran M. I.; Murdoch P. D. S.; Ranford, J. O. Sadler, P. J. *Inorg. Chem.* **1996**, *35*, 1065. (b) Barnham, K. J.; Djuran M. I.; Frey, U.; Mazid, M. A.; Sadler, P. J. *J. Chem. Soc., Chem Commun* **1994**, 65. (c) Alessio, E.; Mestroni, G.; Bergamo, A.; Sava, G. *Met. Ions Biol. Syst.* **2004**, 323−351. (d) Alessio, E.; Mestroni, G.; Bergamo, A.; Sava, G. *Curr. Top. Med. Chem.* **2004**, *4*, 1525−1535. (e) Redemaket-Lakhai, J. M.; van den Bongard, D.; Pluim, D.; Beijnen, J. H.; Schellens, J. H. M. *Clin. Cancer Res.* **2004**, *10*, 3717. (f) Hotze, A. C. G.; Bacac, M.; Velders, A. H.; Jansen, B. A. J.; Kooijman, H.; Spek, A. L.; Haasnnoot, J. G.; Reedijk, J. *J. Med. Chem.* **2003**, *46*, 1743.

(16) See, for example: (a) Moulton, B.; Zaworotko, M. J. *Chem. Rev.* **2001**, *101*, 1629. (b) Batten, S. R. *CrystEngComm* **2001**, *3*, 67. (c) James, S. L. *Chem. Soc. Rev.* **2003**, *32*, 276 and references therein.

(17) Very recently, a similar 1D system has been reported; see: Rzączyńska, Z.; Bartyzel, A.; El×c0bieta O.; Dobrowolska, W.-S. *Polyhedron* **2006**, *25*, 687.

was added dropwise to a warm aqueous suspension (75 cm^3) of basic copper(II) carbonate (0.221 g, 1 mmol) under continuous stirring and heating below 70 °C in a water bath. The mixture was heated for an additional 2 h and then filtered to remove any undissolved starting material. The resulting blue solution was left to evaporate. After a few days a blue crystalline powder was obtained. The product was filtered out, washed with ethanol and ether, and air-dried; yield, 80%. Anal. Calcd (found) for C$_6$H$_8$CuO$_5$ (M_r = 223.66): C, 32.22 (32.10); H, 3.61 (3.55). Selected IR data (KBr, cm^{-1}): 3672 (m), 3543 (m), 1643 (vs), 1574 (vs), 1531 (vs), 1476 (m), 1445 (m), 1375 (s), 1228 (w), 1158 (w), 1141(w), 912 (w), 788 (w), 703 (w), 667 (w), 597 (w), 497 (w), 424 (w).

Method B. A solution of H$_2$cbdca (0.144 g, 1 mmol) in water (10 cm^3) was mixed with a solution of Cu(ClO$_4$)$_2$·6H$_2$O (0.371 g, 1 mmol) in water (15 cm^3). The solution of 0.1 M NaOH was then added drop by drop until the pH reached 6. The blue solution was filtered to remove any impurity and left to slowly evaporate. After 1 week, dark blue crystals suitable for X-ray determination were obtained. The product was identified by analysis and IR comparison with the product from method A.

[Cu$_2$(μ-cbdca)$_2$(μ-bipy)$_2$]$_n$ (2) and [Cu(μ-cbdca)(μ-bpe)]$_n$ (3). Method A. An ethanolic solution (5 cm^3) of 4,4′-bipyridine (0.156 g, 1 mmol) or 1,2-bis(4-pyridyl)ethane (0.184 g, 1 mmol) for **2** and **3**, respectively, was added to an aqueous solution of **1** (0.223 g, 1 mmol, 50 cm^3). A pale blue precipitate was formed that was collected by filtration and washed with ethanol and ether and then air-dried. The yield was practically quantitative. The insolubility of these compounds in most solvents precludes the preparation of a single crystal for X-ray diffraction by this direct procedure. However, single crystals of **2** and **3** were grown by slow diffusion in a straight glass tube of two solutions containing compound **1** in water and the corresponding amine dissolved in ethanol. The two solutions were separated by 10 cm^3 of THF to afford the slow diffusion. Yield: 85% and 90%, respectively. Anal. Calcd (found) for **2**, C$_{32}$H$_{28}$Cu$_2$N$_4$O$_8$ (M_r = 723.66): C, 53.11 (53.03); N, 7.74 (7.70); H, 3.90 (3.82). Calcd (found) for **3**, C$_{18}$H$_{18}$CuN$_2$O$_4$ (M_r = 389.89): C, 55.45 (55.46); N, 7.18 (7.18) H, 4.65 (4.64). Selected IR data (KBr, cm^{-1}): for **2**, 1613 (vs), 1545 (s), 1414 (m), 1399 (m), 1324 (m), 820 (m); for **3**, 2958 (m), 2935 (m), 1612 (vs), 1543 (vs), 1500 (m), 1456 (m), 1429 (m), 1395 (s), 1351 (m), 1314 (m), 1224 (m), 1028 (m), 835 (s), 758 (m), 548 (s).

Method B. An aqueous solution (10 cm^3) of H$_2$cbdca (0.144 g, 1 mmol) neutralized with 0.1 M NaOH was mixed with a solution of Cu(ClO$_4$)$_2$·6H$_2$O (0.371 g, 1 mmol) in water (15 cm^3) under continuous stirring. An ethanolic solution of 4,4′-bipyridine or 1,2-bis(4-pyridyl)ethane (1 mmol, 5 cm^3) was added dropwise to the aqueous one. A pale blue precipitate of **2** and **3** was formed immediately. The products were identified by analysis and IR comparison with products from method A.

[Cu(μ-cbdca)(bpy)]$_2$ (4) and [Cu(cbdca)(phen)(H$_2$O)]·2H$_2$O (6). Complexes **4** and **6** were obtained by using 2,2′-bipyridine (0.156 g, 1 mmol) for **4** and 1,10-phenanthroline monohydrate (0.198 g, 1 mmol) for **6** instead of 4,4′-bipyridine and applying the two methods described above. Single crystals suitable for X-ray diffraction were obtained by slow evaporation at room temperature from the mother liquor of method A; yield 70% and 76%, respectively. Anal. Calcd (found) for **4**, C$_{16}$H$_{14}$CuN$_2$O$_4$ (M_r = 361.83): C, 53.11 (53.03), N, 7.74 (7.72); H, 3.90 (3.88). Calcd (found) for **6**, C$_{18}$H$_{20}$CuN$_2$O$_7$ (M_r = 439.90): C, 49.14 (49.13), N, 6.37 (6.36); H, 4.58 (4.59). Selected IR data (KBr, cm^{-1}): for **4**, 1651 (vs), 1626 (s), 1605 (m), 1475 (w), 1450 (w), 1350 (s), 1121 (w), 780 (m); for **6**, 3474 (s), 1627 (m), 1597 (vs), 1559 (s), 1517 (s), 1427 (s), 1416 (s), 1343 (m), 724 (s).

[Cu(terpy)(ClO$_4$)]$_2$(μ-cbdca)·H$_2$O (5). Compound **5** was obtained by applying method B only and using an ethanolic solution of 2,2′:6′,2″- terpyridine (0.233 g, 1 mmol, 10 cm^3). Small green crystals were obtained from the undisturbed solution after several days; yield 76%. Anal. Calcd (found) for C$_{36}$H$_{32}$Cl$_2$Cu$_2$N$_6$O$_{14}$ (M_r = 952.64): C, 45.38 (45.40); N, 8.82 (8.81); H, 3.17 (3.15). Selected IR data (KBr, cm^{-1}) for **5**: 3435 (m), 1596 (s), 1576 (vs), 1558 (m), 1473 (s), 1449 (m), 1387 (m), 1363 (m), 1140 (s), 1116 (vs), 1091 (vs), 1021 (m), 781 (s), 636 (w), 626 (m).

Physical Measurements. Elemental analyses (C, H, and N) were carried out by the "Serveis Científico-Tècnics" of the University of Barcelona. Infrared spectra (400−4000 cm^{-1}) were recorded from KBr pellets on a Nicolet 5700 FT-IR spectrophotometer. Magnetic measurements were performed at the "Servei de Magnetoquímica" of the University of Barcelona on polycrystalline samples with a Quantum Design SQUID MPMS-XL susceptometer working in the 2−300 K range and operating at 100 G ($T < 50$) and 1000 G (over the whole temperature range). The diamagnetic corrections were evaluated from Pascal's constants. Experimental susceptibilities were also corrected for the temperature-independent paramagnetism (60 × 10^{-6} cm^3 mol^{-1}/Cu(II)). The fits were performed by minimizing the function $R = \Sigma(\chi T_{Mexp} - \chi T_{Mcal})^2/\Sigma(\chi T_{Mexp})^2$.

Crystal Data Collection and Refinement. A similar but slightly different method was used to determine the crystal structure of the six new compounds. Suitable single crystals of **1** and **6** were mounted on a Enraf-Nonius CAD4 four-circle diffractometer. Unit-cell parameters were determined from automatic centering of 25 reflections ($12 \leq \theta \leq 21°$) and refined by the least-squares method. Intensities were collected with graphite-monochromatized Mo Kα radiation using the $\omega/2\theta$ scan technique. Three reflections were measured every 2 h as orientation and intensity control; significant intensity decay was not observed. The selected crystals of **2**, **3**, and **5** were mounted on a MAR345 diffractometer with an image plate detector. Unit-cell parameters were determined from 8327 (in **2**), 90 (in **3**), and 124 (in **5**) reflections ($3 \leq \theta \leq 31°$) and refined by the least-squares method. Intensities were also collected with graphite-monochromatized Mo Kα radiation using the ϕ scan technique. Every image was collected turning ϕ only 1°. Crystal **4** was mounted on a Bruker SMART-CCD area diffractometer with graphite-monochromatized Mo Kα radiation. Each frame covered 0.3° in ϖ, and the first 50 frames were recollected at the end of data collection to monitor crystal decay. Lorentz−polarization correction was made for all compounds while absorption corrections were only made for **1**−**4** using the SADABS program.[18] All structures were solved by direct methods and refined by a full-matrix least-squares method on F^2. The computer programs used were SHELXS-97[19] and SHELXL-97,[19] respectively. Four carbon atoms of **3** and a water molecule of **5** were located in disorder sites; an occupancy factor of 0.5 was assumed for each site according to results from the refinement of occupancy factor. Three H's of **1** and five H's of **2** were located from a difference synthesis, while 23, 24, 14, 28, and 14 H's of **2**−**6**, respectively, were computed. The computed H atoms were refined using a riding model, and all H atoms were refined with an isotropic temperature coefficient equal to 1.2 times the equivalent temperature factor of the linked atoms. The final geometric calculations and graphical manipulations were carried out with the PLATON[20] program. Crystal data and experimental conditions are summarized in Table 1.

(18) Sheldrick, G. M. *SADABS*, version 2.10; Bruker AXS Inc.: Madison, WI, 2003.
(19) Sheldrick, G. M. *SHELX97, Programs for Crystal Structure Analysis*, release 97-2; Institüt für Anorganische Chemie der Universtät: Göttingen, Germany, 1998.
(20) PLATON: Spek, A. L. *Acta Crystallogr.* **1990**, *A46*, C-34.

Table 1. Crystal Data and Structure Refinement for [Cu(μ-cbdca)(H$_2$O)]$_n$ (**1**), [Cu$_2$(μ-cbdca)$_2$(μ-bipy)$_2$]$_n$ (**2**), [Cu(μ-cbdca)(μ-bpe)]$_n$ (**3**), [Cu(μ-cbdca)(bpy)]$_2$ (**4**), [Cu(terpy)(ClO$_4$)]$_2$(μ-cbdca·H$_2$O (**5**), and [Cu(phen)(cbdca)(H$_2$O)]·2H$_2$O (**6**)

| param	1	2	3	4	5	6
formula	C$_6$H$_8$CuO$_5$	C$_{32}$H$_{28}$Cu$_2$N$_4$O$_8$	C$_{18}$H$_{18}$CuN$_2$O$_4$	C$_{32}$H$_{28}$CuN$_4$O$_8$	C$_{36}$H$_{30}$Cl$_2$Cu$_2$N$_6$O$_{13}$	C$_{18}$H$_{20}$CuN$_2$O$_7$
fw	223.65	723.66	389.85	723.66	952.64	439.90
space group	*Pcmn*	*P2$_1$/n*	*P2$_1$/c*	*P$\bar{1}$*	*P$\bar{1}$*	*P2$_1$/c*
a, Å	5.524(6)	17.2910(10)	13.197(7)	8.6090(8)	9.364(6)	9.445(3)
b, Å	7.069(2)	11.1310(10)	14.137(7)	9.9309(9)	9.435(4)	12.135(3)
c, Å	18.501(8)	17.3070(10)	9.161(6)	10.3457(9)	23.362(11)	16.302(15)
α, deg	90	90	90	93.616(2)	80.44(3)	90
β, deg	90	117.8410(10)	94.92(3)	113.762(2)	89.78(3)	102.41(6)
γ, deg	90	90	90	11.153(2)	87.98(3)	90
V, Å^3	722.4	2945.4(4)	1702.8(17)	732.11(11)	2034.1(18)	1824.8(18)
Z	4	4	4	1	2	4
ρ_{calcd}, g/cm^3	2.038	1.632	1.497	1.1641	1.555	1.601
T, °C	20(2)	20(2)	20(2)	25(2)	20(2)	20(2)
λ(Mo Kα), Å	0.710 69	0.710 73	0.710 73	0.710 73	0.710 73	0.170 69
μ(Mo Kα), cm^{-1}	29.98	15.05	13.07	15.14	12.48	12.42
R1^a	0.0356	0.0361	0.0595	0.0383	0.0410	0.0641
wR2^b	0.0700	0.0879	0.1647	0.0861	0.1141	0.0959

Results and Discussion

Description of the Structure of [Cu(μ-cbdca)(H$_2$O)]$_n$ (1). Compound **1** has a sheetlike arrangement of (aqua)-copper(II) units bridged by cbdca ligands growing in the *ab* plane (Figure 1). Each cbdca dianion is coordinated to a copper atom as a bidentate ligand through two oxygen atoms of the two carboxylate fragments, and it is also coordinated to two other neighboring copper atoms in a bis(monodentate) fashion through the free O1. In this way, each cbdca dianion links three Cu(II) atoms related by an axis. The copper atom exhibits a perfect square-pyramidal environment ($\tau = 0$), with the four carboxylate oxygen atoms in the equatorial positions and a water molecule in the axial one. The Cu–O$_{(water)}$ distance of 2.425(4) Å is significantly longer than the average Cu–O$_{(carboxyl)}$ distances of 1.947(2) Å. Each cbdca ligand forms a six-membered chelate ring at the copper atom, the value of the angle subtended at the metal atom being 89.75(14)°. The carboxylate group adopts the *syn-anti* coordination mode, the value of Cu···Cu separation through this bridge being 4.842(5) Å. The dihedral angle between the basal planes of the consecutive Cu(II) units was found to be 82.3(8)°. The ORTEP drawing is shown in Figure 2. Selected interatomic bond distances and angles are listed in Table 2.
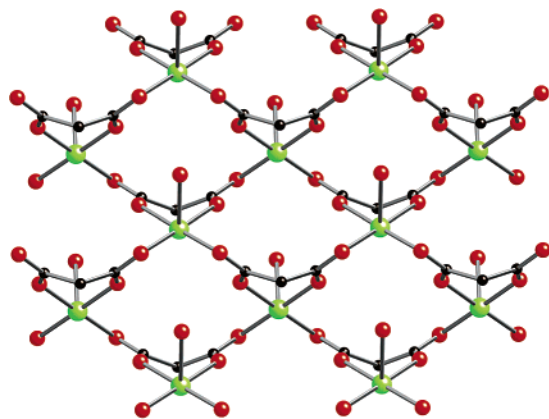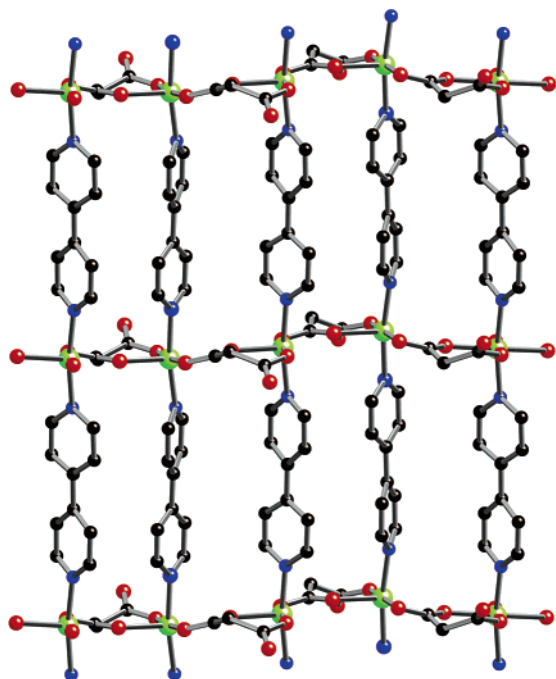

Figure 1. Perspective view of the *ab* plane of the infinite two-dimensional layer sheet structure of compound **1**. The cyclobutane rings are omitted for clarity.

Table 2. Selected Bonds Lengths (Å) and Angles (deg) for [Cu(μ-cbdca)(H$_2$O)]$_n$ (**1**)^a

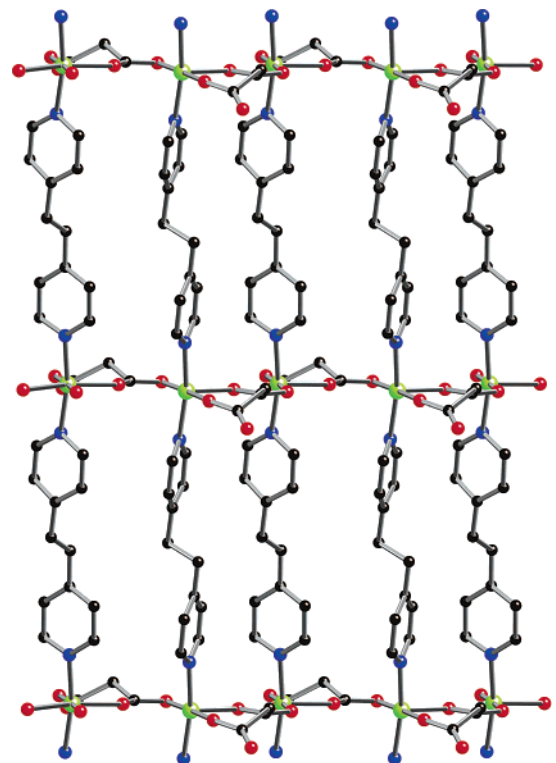|			
Cu–O1	1.952(2)	Cu–O3	2.425
Cu–O2$^{\#1}$	1.943(2)		
O2$^{\#1}$–Cu–O2$^{\#2}$	89.75(14)	O1–Cu–O1$^{\#3}$	90.65(14)
O2$^{\#1}$–Cu–O1	179.28(11)	O2$^{\#1}$–Cu–O3	89.55(11)
O2$^{\#2}$–Cu–O1	89.80(9)	O1–Cu–O3	89.88(11)

^{a} Symmetry transformations used to generate equivalent atoms: #1, $x - 1/2$, $y + 1/2$, $-z + 1/2$; #2, $x - 1/2$, $-y$, $-z + 1/2$; #3, x, $-y + 1/2$, z; #4, $x + 1/2$, $y - 1/2$, $-z + 1/2$; #5, x, $-y - 1/2$, z.
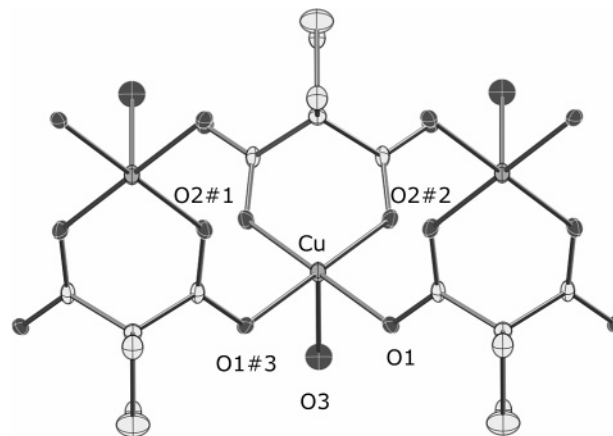
Figure 2. Molecular fragment of compound **1** with the numbering scheme. The ellipsoids are drawn at the 30% probability level. The numbering of the carbon atoms is omitted for clarity.

Description of the Structures of [Cu$_2$(μ-cbdca)(μ-bipy)]$_n$ (2) and [Cu(μ-cbdca)(μ-bpe)]$_n$ (3). The crystal structures of **2** and **3** consist of polymeric neutral sheets involving chains of cbdca and metal ions linked by 4,4′-bipyridine and 1,2-bis(4-pyridyl)ethane ligands, respectively (Figures 3 and 4). Each cbdca group simultaneously adopts chelate (through O1 and O3 atoms toward Cu1 and O5 and O7 atoms toward Cu2 for compound **2** and through O1 and O3 for compound **3**) and monodentate (through O4 and O9 atoms toward Cu2 and Cu1, respectively, for **2** and through O2 for **3**) coordination modes. Two slightly different carboxylate bridges (O3–C13–O4 and O7–C27–O9) that adopt a *syn-anti* conformation and link an equatorial with an axial copper site alternate regularly within each chain in

Figure 3. View of the layer of the complex **2**. The bipy ligand connects chains of carboxylate-bridged copper(II) ions. The cyclobutane rings and hydrogen atoms are omitted for clarity.
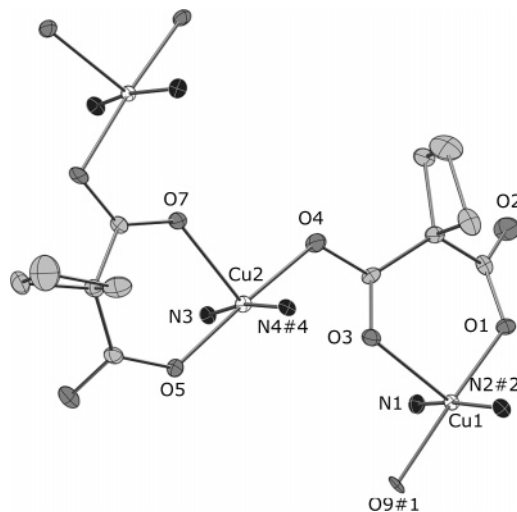

Figure 4. View of the layer of the complex **3**. The bpe ligand connects chains of carboxylate-bridged copper(II) ions. The cyclobutane rings and hydrogen atoms are omitted for clarity.
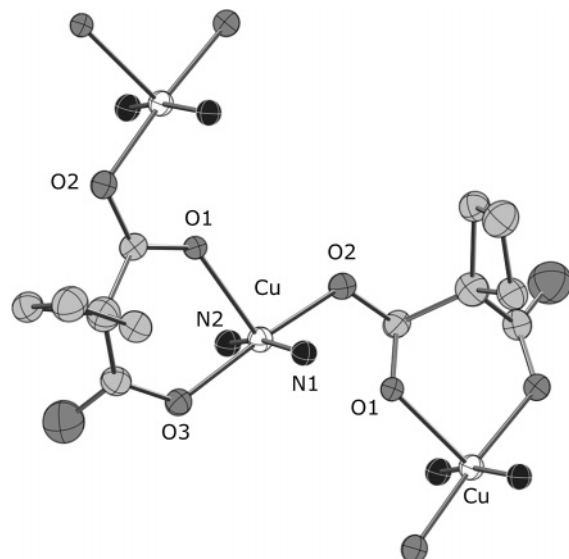

Figure 5. View of a fragment of the carboxylate-bridged copper(II) chains of compound **2** with the numbering scheme. The ellipsoids are drawn at the 30% probability level. The bipy rings and numbering of the carbon atoms are omitted for clarity.

average H···centroid lengths equal to 3.29 Å. The two crystallographically independent copper(II) ions (Cu1 and Cu2) in **2** and the single copper (II) ion in **3** exhibit a distorted CuN_2O_3 square pyramidal geometry, the geometric τ factor being 0.1 for all ions. Two nitrogen atoms from two 4,4′-bipyridine groups and two carboxylate oxygen atoms from two different cbdca's build the basal plane, the mean value of Cu−O bonds (1.9594 Å for **2** and 1.928 Å for **3**) being somewhat shorter than that of the Cu−N (2.0457 Å for **2** and 2.005 Å for **3**) ones. A carboxylate oxygen from a bidentate cbdca occupies the apical position for both Cu atoms; the Cu−O bond lengths are 2.1415(18) Å for Cu1 and 2.1351(18) Å for Cu2 for compound **2** and 2.147(3) Å for compound **3**. The Cu1 and Cu2 atoms deviate by 0.124 and 0.112 Å, respectively, from the basal plane toward the apical carbonyl O atom for **2** and 0.137 Å for **3**. The ORTEP drawings are shown in Figures 5 and 6. Selected interatomic bond distances and angles are listed in Tables 3 and 4.

Description of the Structure of [Cu(μ-cbdca)(bpy)]₂ (4). The structure consists of a centrosymmetric dinuclear [Cu(μ-cbdca)(bpy)]₂ molecule in which the Cu atoms are coordinated by two N atoms from one 2,2′-bipyridine ligand and three O atoms from two cbdca ligands to form a slightly distorted [CuN_2O_3] square pyramid ($\tau = 0.13$). The pyridyl N atoms and carboxyl O atoms of one cbdca ligand form the basal plane, while the apical position is occupied by one carboxyl oxygen atom from the second dicarboxylate ligand. Two adjacent [CuN_2O_3] square pyramids are edge-shared via two μ_2 carboxyl O atoms. The Cu−N bond distances average 1.992 Å, the basal Cu−O bond distances average 1.969 Å, and the axial Cu−O bond length is 2.3149(19) Å. The bridging Cu_2O_2 is strictly planar owing to the inversion center, with a Cu···Cu separation of 3.243(8) Å. The value of the angle at the oxo bridge Cu−O−Cu is 98.76(7)°. The Cu atom is shifted 0.155 Å from the mean basal plane toward the apical oxygen atom. The ORTEP drawing is shown in Figure 7. Selected interatomic bond distances and angles are listed in Table 5.

compound **2**, whereas only one type of carboxylate bridge (O2−C1−O1) appears in **3** with the same conformation. The values of Cu···Cu separation through these bridges are 4.7474(6) and 4.7567(6) Å for **2** and 4.815(3) Å for **3**. The alternating localization of 4,4′-bpy and cbdca ligands along the chain in **2** produces C−H···π ring interactions with

Figure 6. Fragment of the uniform chain of compound **3** showing the numbering scheme. The ellipsoids are drawn at the 30% probability level. The bpe rings and numbering of the carbon atoms are omitted for clarity.

Table 3. Selected Bonds Lengths (Å) and Angles (deg) for [Cu₂(μ-cbdca)₂(μ-bipy)₂]ₙ (**2**)ᵃ

|			
Cu1−O1	1.9149(18)	Cu2−O5	1.9380(18)
Cu1−O9#1	1.9995(16)	Cu2−O4	1.9853(19)
Cu1−N2#2	2.047(2)	Cu2−N4#2	2.0320(19)
Cu1−N1	2.065(2)	Cu2−N3	2.039(2)
Cu1−O3	2.1415(18)	Cu2−O7	2.1351(18)
O1−Cu1−O9#1	175.62(7)	O5−Cu2−O4	176.52(8)
O1−Cu1−N2#2	90.19(8)	O5−Cu2−N4#2	90.21(8)
O9#1−Cu1−N2#2	92.35(8)	O4−Cu2−N4#2	90.79(9)
O1−Cu1−N1	87.15(8)	O5−Cu2−N3	88.06(9)
O9#1−Cu1−N1	89.71(8)	O4−Cu2−N3	90.41(9)
N2#2−Cu1−N1	169.40(9)	N4#2−Cu2−N3	170.49(9)
O1−Cu1−O3	91.42(7)	O5−Cu2−O7	91.79(7)
O9#1−Cu1−O3	91.80(7)	O4−Cu2−O7	91.39(7)
N2#2−Cu1−O3	97.06(9)	N4#2−Cu2−O7	97.13(9)
N1−Cu1−O3	93.26(9)	N3−Cu2−O7	92.28(9)

ᵃ Symmetry transformations used to generate equivalent atoms: #1, $x − 1/2, −y + 1/2, z − 1/2$; #2, $x, y − 1, z$; #3, $x + 1/2, −y + 1/2, z + 1/2$; #4, $x, y + 1, z$.

Table 4. Selected Bonds Lengths (Å) and Angles (deg) for [Cu(μ-cbdca)(μ-bpe)]ₙ (**3**)ᵃ

Cu−O2#1	1.882(3)	Cu−N1#2	2.013(3)
Cu−O3	1.974(3)	Cu−O1	2.147(3)
Cu−N2	1.998(3)		
O2#1−Cu−O3	175.51(10)	N2−Cu−N1#2	168.78(13)
O2#1−Cu−N2	89.72(11)	O2#1−Cu−O1	95.82(9)
O3−Cu−N2	89.75(11)	O3−Cu−O1	88.67(9)
O2#1−Cu−N1#2	89.56(10)	N2−Cu−O1	95.13(11)
O3−Cu−N1#2	90.10(10)	N1#2−Cu−O1	96.09(11)

ᵃ Symmetry transformations used to generate equivalent atoms: #1, $x, −y − 1/2, z + 1/2$; #2, $x − 1, y, z$; #3, $x, −y − 1/2, z − 1/2$; #4, $x + 1, y, z$; #5 $−x, −y, −z − 1$.

Description of the Structure of [Cu(terpy)(ClO₄)]₂(μ-cbdca)·H₂O (5). The structure of complex **5** consists of neutral dinuclear Cu(II) cations bridged via the dicarboxylate oxygen atoms in bis(unidentate) mode. This unit is depicted in Figure 8, together with the numeric scheme. Selected distances and angles are listed in Table 6. The coordination geometry about each copper(II) can be adequately described as distorted square pyramidal ($\tau = 0.25$ for Cu1 and 0.21
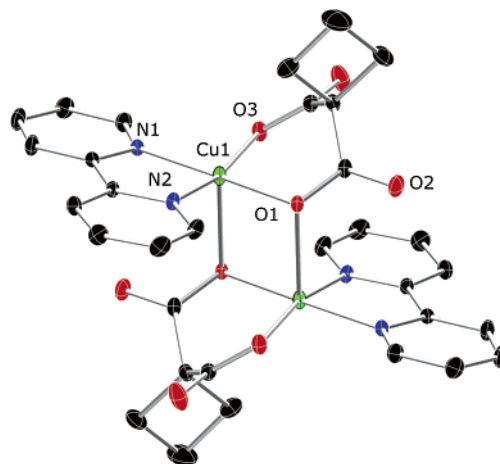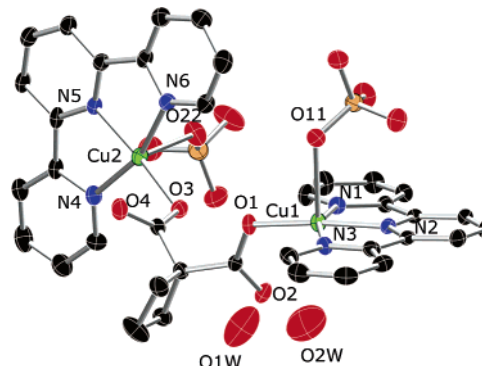

Figure 7. ORTEP 30% probability diagram of compound **4**. Hydrogen atoms and numbering of the carbon atoms are omitted for clarity.

Table 5. Selected Bonds Lengths (Å) and Angles (deg) for [Cu(μ-cbdca)(bpy)]₂ (**4**)ᵃ

Cu1−O3	1.9327(19)	Cu1−N2	2.007(2)
Cu1−O1	1.9464(18)	Cu1−O1#1	2.3149(19)
Cu1−N1	1.977(2)		
O3−Cu1−O1	91.73(8)	O3−Cu1−O1#1	97.74(8)
O3−Cu1−N1	93.38(9)	O1−Cu1−O1#1	81.24(8)
O1−Cu1−N1	174.09(9)	N1−Cu1−O1#1	100.98(8)
O3−Cu1−N2	165.95(9)	N2−Cu1−O1#1	95.94(8)
O1−Cu1−N2	93.53(8)	Cu1−O1−Cu1#1	98.76(8)
N1−Cu1−N2	80.82(9)		

ᵃ Symmetry transformations used to generate equivalent atoms: #1, $−x + 1, −y + 1, −z + 2$.

Figure 8. ORTEP 30% probability diagram of the asymmetric unit of **5** with the atom numbering. O1W and O2W are the disordered sites of the hydrate water molecule.

for Cu2), with the perchlorate oxygen atoms occupying the apical positions. As expected, the axial bonds are longer than the bond lengths in the basal plane ($Cu−O_{perchlorate} = 2.441(3)$ and 2.398(3) Å for Cu1 and Cu2, respectively). Three nitrogen atoms from terpy and one oxygen atom from the unidentate bridged cbdca ligand comprise the basal plane, the main value of Cu−N bonds (2.004 Å for Cu1 and 1.998 Å for Cu2) being somewhat longer than that of the Cu−O (1.916 Å for Cu1 and 1.929 Å for Cu2). The Cu1···Cu2 distance is 6.074(4) Å. The main crystallographic feature is the unidentate behavior of each carboxylate group. In this coordination mode one oxygen atom from each carboxylate group bond with a different metal as unidentate, while the remaining oxygen remains uncoordinated. This coordination
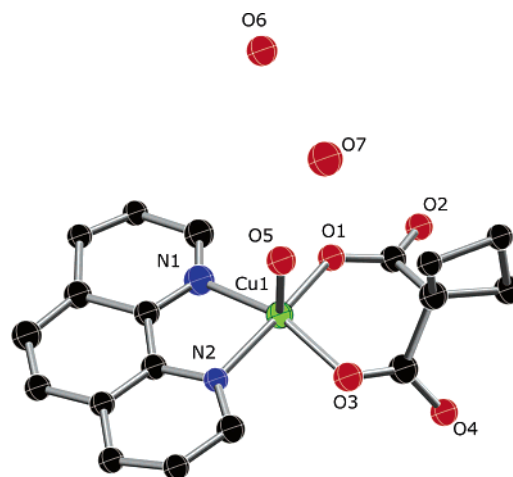
Table 6. Selected Bonds Lengths (Å) and Angles (deg) for [Cu(terpy)(ClO$_4$)]$_2$(μ-cbdca)·H$_2$O (**5**)

Cu1−O1	1.9156(19)	Cu2−O3	1.929(2)
Cu1−N2	1.937(2)	Cu2−N5	1.949(2)
Cu1−N1	2.029(3)	Cu2−N6	2.019(3)
Cu1−N3	2.045(3)	Cu2−N4	2.027(3)
Cu1−O11	2.441(1)	Cu2−O22	2.398(3)
O1−Cu1−N2	175.02(11)	O3−Cu2−N5	172.71(10)
O1−Cu1−N1	101.89(11)	N5−Cu2−N6	79.93(12)
N2−Cu1−N1	80.13(10)	O3−Cu2−N4	98.47(13)
O1−Cu1−N3	97.32(10)	N5−Cu2−N4	81.07(13)
N2−Cu1−N3	80.29(10)	N6−Cu2−N4	160.61(10)
N1−Cu1−N3	160.01(9)	O3−Cu2−O22	94.46(11)
O11−Cu1−N3	92.35(13)	N5−Cu2−O22	92.80(11)
O11−Cu1−N2	93.49(13)	N4−Cu2−O22	97.54(13)
O11−Cu1−N1	92.78(13)	N6−Cu2−O22	87.25(14)
O11−Cu1−O1	90.99(11)	O3−Cu2−N6	99.88(11)

mode only appears in two infinite helical chains with Zn as a metal and malonate[21] and ethylmalonate[22] as the bridging ligand and in two other polymer compounds[23,24] where the malonate bridge alternates with other bridges. In all cases the crystal structures are stabilized by an extensive network of intra- and interlayer hydrogen bonds. Recently, Bratsos et al.[25] reported a dinuclear compound with Ru(II), where for the first time the cbdca presented this coordination mode. In this compound the two metal centers are bridged by two carboxylate groups and present the ancillary ligands capable of making intramolecular H-bonds with the noncoordinated oxygen atoms of the carboxylate groups. The authors argue that the short interligand H-bond is the driving force that induces cbdca to act as a bridging rather than a chelating ligand. In contrast, in compound **5** the two metal centers are bridged by only one carboxylate group and there are no H-bonds between the oxygen atoms from perchlorate or carboxylate groups and water molecules. In contrast, $\pi-\pi$ stacking interactions occur between pyridine rings of terpyridine ligands, the average centroid⋯centroid distance being 3.640 Å (range: 3.556−3.709 Å). This interaction produces zigzag chains of dinuclear units along the $a-c$ axis.

Description of the Structure of [Cu(cbdca)(phen)-(H$_2$O)]·2H$_2$O (6). The crystal structure of complex **6** consists of a neutral [Cu(cbdca)(phen)(H$_2$O)] molecule and two lattice water molecules. Figure 9 shows a perspective view of the molecular structure with atom labeling. The selected bond lengths and angles are listed in Table 7. The copper atom exhibits a distorted square pyramidal environment, where the geometrical τ value is 0.2. The Cu(II) is bonded to two phen nitrogen atoms [1.982(9) and 2.013(7) Å for Cu−N1 and Cu−N2, respectively] and two carboxylate oxygen atoms from the cbdca group [1.918(6) and 1.923(7) Å for Cu−O1 and Cu−O3, respectively] in the basal plane and to an oxygen atom from the water molecule in the apical position

Figure 9. View of the molecular structure of complex **6** with 20% displacement ellipsoids probability.

Table 7. Selected Bonds Lengths (Å) and Angles (deg) for [Cu(cbdca)(phen)(H$_2$O)]·2H$_2$O (**6**)

Cu1−O1	1.918(6)	Cu1−N2	2.013(7)
Cu1−O3	1.923(7)	Cu1−O5	2.226(7)
Cu1−N1	1.982(9)		
O1−Cu1−O3	94.2(3)	N1−Cu1−N2	80.9(4)
O1−Cu1−N1	90.8(4)	O1−Cu1−O5	99.4(3)
O3−Cu1−N1	155.2(4)	O3−Cu1−O5	102.5(3)
O1−Cu1−N2	167.1(3)	N1−Cu1−O5	100.6(4)
O3−Cu1−N2	89.4(3)	N2−Cu1−O5	91.9(3)

[2.226(7) Å for Cu−O5]. The angle between the phen (nitrogen atoms) and the metal ion is far from the ideal value of 90° [80.90(4)° for N1−Cu− N2] because of the geometrical constraints imposed by the phen ligand. The copper atom is displaced 0.317 Å from the mean basal plane toward to the apical position.

The O5 water molecule linked to the Cu ion acts as a donor in two hydrogen bonds to the carboxylate O4 atom (2.721(10) Å) and to the O6 water molecule (2.718(10) Å). O6 acts as a donor in two hydrogen bonds to the carboxylate O2 atom (2.875(10) Å) and the O7 water molecule (2.700(10) Å), and O7 acts as a donor in two hydrogen bonds to the two carboxylate O2 and O4 atoms [2.886(12) and 2.890(11) Å, respectively; Figure 10]. This scheme of hydrogen bonds
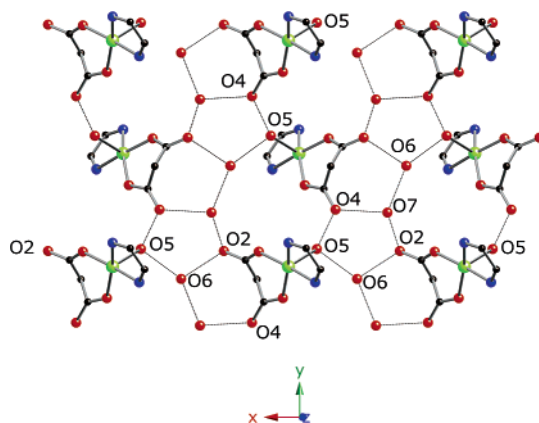
Figure 10. 2D hydrogend-bonden network (dashed line) of **6** involving the coordinated and crystallization water molecules and the carboxylate oxygen atoms. The cyclobutane and phen rings have been omitted for clarity.

(21) Burrows, A. D.; Harrington, R. W.; Mahon, M. F.; Price, E. C. *J. Chem. Soc., Dalton Trans.* **2000**, 3845.
(22) Burrows, A. D.; Donovan, A. S.; Harrington, R. W.; Mahon, M. F. *Eur. J. Inorg. Chem.* **2004**, 4686.
(23) Hong, S. C.; Kim, J.; Hur, N. H.; Do, Y. *Inorg. Chem.* **1996**, *35*, 5110−5111.
(24) Zhao, W.; Fan, J.; Okamura, T.; Sun, W.-Y.; Ueyama, N. *J. Solid State Chem.* **2004**, *177*, 2358.
(25) Bratsos, I.; Zangrando, E.; Serli, B.; Katsaros, N.; Alessio, E. *Dalton Trans.* **2005**, 3881−3885.

produces a chain of mononuclear entities along the *a* axis through the O5 coordinated water molecule to the O6 uncoordinated water molecule of the same asymmetric unit and O2 of the uncoordinated carboxylate from another molecule. Another chain perpendicular to the first one is produced along the *b* axis through an O4 uncoordinated carboxylate oxygen atom from one mononuclear unit and the O5 coordinate water molecule to another mononuclear one. In addition, the remaining O7 uncoordinated water molecule links O2 and O6 from two parallel chains along the *a* axis and, simultaneously, an O4 from the chain parallel to the *b* axis. Furthermore, $\pi-\pi$ stacking interactions are present between phen rings, the average centroid···centroid distance being 3.662 Å (range: 3.526−3.732 Å) and the parallel displacement angle being 2.99°, in agreement with previously reported values.[26] The two intermolecular interactions (hydrogen bonds and π interactions) build an extended two-dimensional network parallel to the *ab* plane.

Magnetic Properties. Complex 1. The magnetic properties of complex **1** in the form $\chi_M T$ vs T [χ_M being the molar magnetic susceptibility/copper(II) ion] are shown in Figure 11. $\chi_M T$ at room temperature is 0.44 cm^3 mol^{-1} K, a value which is as expected for a magnetic isolated spin doublet (g = 2.16). This value continuously increases when the sample is cooling and increases sharply below 14 K, reaching a value of 3.45 cm^3 mol^{-1} K at 2 K. This feature is indicative of an overall weak ferromagnetic coupling between the copper(II) ions.

As indicated in the structural section, complex **1** is a two-dimensional net in which each Cu(II) ion is linked to four different Cu(II) through carboxylate bridges in *syn-anti* fashion. Due to symmetry of the structure, only one *J* value is necessary to interpret the magnetic results. The exchange parameter *J* has thus been obtained by fitting the magnetic data to the expression for the susceptibility derived by Baker et al.[27] from high-temperature series expansion results for an isotropic ferromagnetic quadratic lattice with spin S = 1/2. The series takes the following form:

$$\chi_M = \frac{Ng^2\beta^2}{k_B T}\left[1 + \sum_{n\geq 1}\frac{\alpha_n}{2^n n!}x^n\right]$$

Here n = integer values from 1 to 10, $x = J/k_B T$, and α_n is the coefficient for the square lattice. For S = 1/2, the α_n values are know up to n = 10. The best fit parameters are J = 4.76 cm^{-1}, g = 2.14, and R = 8.7 × 10^{-4} (R previously defined).

The value of the superexchange parameter *J* for **1** is comparable with magnetic data found in the literature for other *syn-anti* carboxylate-bridged copper(II) complexes with d$_{x^2-y^2}$ magnetic orbitals and carboxylate bridges linking two basal positions.[28] As pointed out by several authors[28k,l] for *syn-anti* Cu−O−C−O−Cu complexes, the contributions from the 2p orbitals of O atoms belonging to the magnetic orbitals centered on Cu(II) ions are unfavorably oriented to
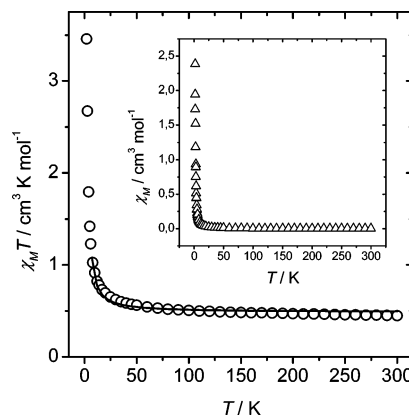
Figure 11. Experimental temperature dependence of the $\chi_M T$ product (χ_M being the magnetic susceptibility/Cu(II) ion) for complex **1**. The solid line represents the best fitting (see text for the fitted parameters). The inset shows the thermal dependence of the χ_M.

give a significant overlap; therefore, a weak magnetic coupling is observed. The nonplanarity of the Cu−O−C−O−Cu skeleton, in which the dihedral angle is 82.3° (see structural part), is also expected to reduce the overlap of the magnetic orbitals in the bridging region, which decreases the antiferromagnetic contribution, and as a result the ferromagnetic term becomes dominant.[28c−k] This ferromagnetic term will be the greatest for a dihedral angle of 90°. Indeed, theoretical DFT calculations also corroborate this weak ferromagnetic coupling for this kind of "nearly perpendicular" *syn-anti* conformation.[29]

Furthermore, the experimental *J* value is an average between the J_F *syn-anti* magnetic pathway (predominant) and the small AF contribution due to the long Cu−O−C−C−C−O−Cu pathway, which is not zero, as can be observed in complex **5** (see below). Thus, the actual J_F value will likely be greater than 4.76 cm^{-1}.

Complex 2. The global feature of the $\chi_M T$ vs T curve for complex **2** is shown in Figure 12. The value of $\chi_M T$ at 300 K is 0.435 cm^3 mol^{-1} K, which is as expected for one uncoupled copper(II) ion (g = 2.15). Upon cooling of the sample from room temperature, $\chi_M T$ decreases slightly and reaches a value of 0.410 cm^3 mol^{-1} K at 10 K, whereupon it decreases again down to a value of 0.292 cm^3 mol^{-1} K at

(26) Janiak, *C. J. Chem. Soc., Dalton Trans.* **2000**, 3885.

(27) Baker, G. A.; Gilbert, H. E.; Eve, J.; Rushbrooke, G. S. *Phys. Lett.* **1967**, *25A*, 207−209.

(28) (a) Nanda, K. K.; Addison, A. W.; Sinn, E.; Thompson, L. K. *Inorg. Chem.* **1996**, *35*, 5966. (b) Bakalbassi, E.; Tsipis, C.; Bozopoulos, A.; Dreissing, W.; Harti, H.; Mrozinski, J. *Inorg. Chim. Acta* **1991**, *186*, 113. (c) Colacio, E.; Domínguez-Vera, J. M.; Kivekäs, R.; Moreno, J. M.; Romerosa, A.; Ruiz, J. *Inorg. Chim. Acta* **1993**, *212*, 115. (d) Ruiz-Perez, C.; Sanchiz, J.; Molina, M. H.; Lloret, F.; Julve, M. *Inorg. Chem.* **2000**, *39*, 1363 and references therein. (e) Ruiz-Perez, C.; Hernandez-Molina, M.; Lorenzo-Luis, P.; Lloret, F.; Cano, J.; Julve, M. *Inorg. Chem.* **2000**, *39*, 3845 and references therein. (f) Rodriguez-Martín, Y.; Ruiz-Perez, C.; Sanchiz, J.; Lloret, F.; Julve, M. *Inorg. Chim. Acta* **2001**, *318*, 159. (g) Colacio, E.; Costes, J. P.; Kivekäs, R.; Laurent, J. P.; Ruiz, J. *Inorg. Chem.* **1990**, *29*, 4240. (h) Colacio, E.; Domínguez-Vera, J. M.; Costes, J. P.; Kivekäs, R.; Laurent, J. P.; Ruiz, J.; Sundberg, M. *Inorg. Chem.* **1992**, *31*, 774. (i) Murugesu, M.; Clérac, R.; Pilawa, B.; Mandel, A.; Anson, C. E.; Powell, A. K. *Inorg. Chim. Acta* **2002**, *337*, 328. (j) Towle, D. K.; Hoffmann, S. K.; Hatfield, W. E.; Singh, P.; Chaudhuri, P. *Inorg. Chem.* **1988**, *27*, 394. (k) Colacio, E.; Ghazi, M.; Kivekäs, R.; Moreno, J. M. *Inorg. Chem.* **2000**, *39*, 2882 and references therein. (l) Carling, R. L.; Kopinga, K.; Kahn, O.; Verdaguer, M. *Inorg. Chem.* **1986**, *25*, 1786.

(29) Rodriguez-Fortea, A.; Alemany, P.; Ruiz, E. *Chem.—Eur. J.* **2001**, *7*, 626.
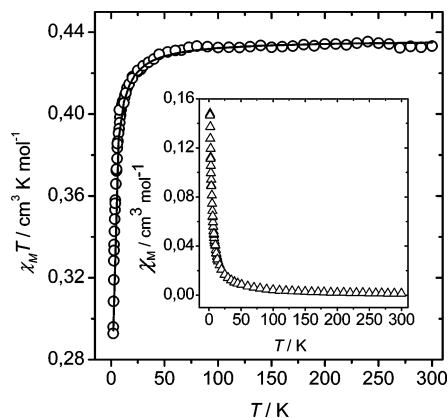
Figure 12. Temperature dependence of the $\chi_M T$ product of **2**: (circles) experimental data; (—) best fit curve (see text). The inset shows the thermal dependence of the χ_M/Cu(II) ion.

Figure 13. Plot of the temperature dependence of the $\chi_M T$ product of **3**. The solid line represent the best theoretical fit. The inset shows the thermal dependence of the χ_M/Cu(II) ion.

2 K. These features are characteristic of a very weak antiferromagnetic interaction.

As commented in the structural section, complex **2** can be considered as formed by two sublattices: a one-dimensional sublattice, formed by Cu(II) ions linked by carboxylate bridging ligands, and these chains linked to one another by a 4,4′-bipy ligand. Taking into account that the bridging ligand 4,4′-bipy always gives a very small (almost negligible) coupling in agreement with the large copper—copper separation (more than 11.1 Å),[30] only the J parameters due to the *syn-anti* carboxylate bridges need be considered. Actually, two J values should be considered owing to the structure in which there are two nonequivalent copper ions. However, the differences between these two copper ions are so small that it is better to consider only one J parameter.

The experimental magnetic data have been fitted using the equation derived from the Bonner—Fisher calculation[31] on the basis of the isotropic Heisenberg Hamiltonian:

$$H = -J\sum_{i}(S_i S_i + 1)$$

The best fit parameters are found as $J = -0.94$ cm^{-1}, $g = 2.16$, and $R = 5.21 \times 10^{-6}$. The low value of the superexchange parameter can be related to the nature of the bridge among the neighboring copper(II) atoms. As in complex **1**, the coupling between the copper atoms is through the carboxylate group of the ligand in *syn-anti* conformation. However, in complex **2** the coordination mode is not basal (short)—basal (short), as in complex **1** but rather the basal (short)—apical (long) coordination mode. This exchange pathway produces a very poor overlap and/or repulsion between the magnetic orbitals due to the weak spin density at the apical site.[8,32] As has been pointed out by Colacio et al.,[28k] when carboxylate groups link copper(II) in *syn-anti* equatorial—axial positions, the coupling through the bridging
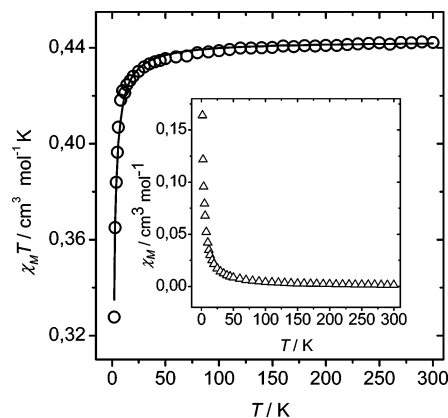
ligand is always very small regardless of the structural parameter of the bridge.

Complex 3. The global feature of the $\chi_M T$ vs T curve for complex **3** is shown in Figure 13. The value of $\chi_M T$ at 300 K is 0.441 cm^3 mol^{-1} K, which is as expected for an uncoupled copper(II) ion ($g = 2.17$). Upon sample cooling from room temperature, $\chi_M T$ decreases slightly and reaches a value of 0.41 cm^3 mol^{-1} K at 10 K, whereupon it decreases again down to a value of 0.33 cm^3 mol^{-1} K at 2 K. These features are characteristic of a very weak antiferromagnetic interaction.

Complex **3** has a structure similar to that of complex **2**; i.e., the coordination mode is *syn-anti* basal (short)—apical (long). It can be considered to be formed by two sublattices, but taking into account that the bridging bpe ligand is larger than the bipy one, only the J parameter due to the *syn-anti* carboxylate bridges need to be considered.

The experimental magnetic data have been fitted as for complex **2**, using the equation derived from the Bonner—Fisher calculation.[31] The best fit parameters are found as $J = -0.67$ cm^{-1}, $g = 2.18$, and $R = 6.02 \times 10^{-6}$. The low value of the superexchange parameter can be related to the nature of the bridge among the neighboring copper(II) atoms. The explanation given for complex **2** is also valid for complex **3**: for both **2** and **3** complexes the τ parameter[10] is the most important one being $\tau = 0.1$ in the two cases. There is, thus, a small—but not negligible— contribution of the d$_{z^2}$ in the magnetic orbital (ca. 10%), which is the responsible of the small AF coupling.

Complex 4. The magnetic properties of complex **4** are shown in Figure 14 in the form of $\chi_M T$ vs T. At room temperature $\chi_M T$ is equal to 0.86 cm^3 mol^{-1} K, the expected value for two magnetically isolated spin doublets ($g = 2.14$), and remains practically constant down to about 90 K; below that temperature this value slowly increases to 0.92 at 9 K and then decreases slightly further. This behavior is typical of a ferromagnetically coupled dinuclear copper(II) complex. The small decrease of $\chi_M T$ in the low-temperature range is due to weak intermolecular magnetic interactions. This decrease might be also due to the ZFS of the $S = 1$ ground state.

(30) (a) Julve, M.; Verdaguer, M.; Faus, J.; Tinti, F.; Moratal, J.; Monge, A.; Gutierrez-Puebla, E. *Inorg. Chem.* **1987**, *26*, 3520. (b) Maji, T. K.; Sain, S.; Mostafa, G.; Lu, T.-H.; Ribas, J.; Monfort, M.; Ray Chaudhuri, N. *Inorg. Chem.* **2003**, *42*, 709.
(31) Bonner, J. C.; Fisher, M. E. *Phys. Rev. A* **1964**, *135*, 640.
(32) Dey, S. K.; Bag, B.; Malik, K. M. A.; El Fallah, M. S.; Ribas, J.; Mitra, S. *Inorg. Chem.* **2003**, *42*, 4029.
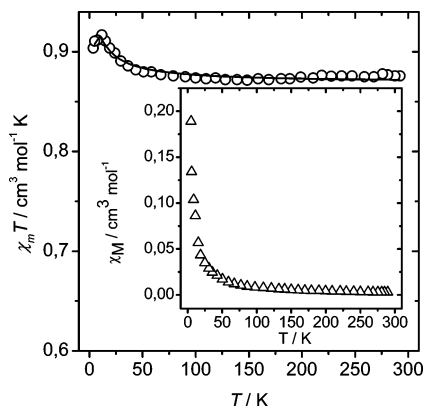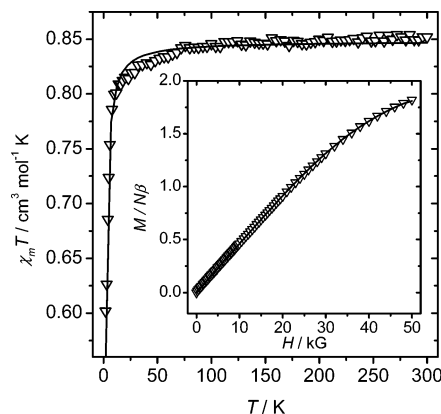
Figure 14. Temperature dependence of the $\chi_M T$ product of **4**. The solid line represents the best theoretical fit. The inset shows the thermal dependence of the $\chi_M/2$ Cu(II) ions.

Figure 15. Experimental temperature dependence of the $\chi_M T$ product (χ_M being the magnetic susceptibility/2 Cu(II) ions) for complex **5**. The inset shows the field dependence of magnetization curve from 0 to 50 kG at 2 K. Solid lines represent the best theoretical fits (see text).

As **4** is a dinuclear copper complex, the susceptibility data were analyzed using the Bleaney−Bowers expression[33] for two magnetically interacting local spin doublets derived from the Hamiltonian $H = -J S_1 \cdot S_2$ and with the inclusion of a $z'J'$ parameter to account for the intermolecular interactions. Least-squares best-fit results are $J = 4.44$ cm^{-1}, $g = 2.14$, $J' = -0.92$ cm^{-1}, and $R = 6 \times 10^{-5}$.

The magnetic pathway in complex **4** is the Cu_2O_2 core (see structural section). The magnetic properties of this core have been exhaustively studied from an experimental and theoretical point of view but only when the two O atoms occupy equatorial−equatorial positions with respect to copper(II) ions. In contrast, the number of similar complexes containing this Cu_2O_2 core with the two O atoms in equatorial−axial positions is rather limited and no general trends have been reported. The magnetic orbital on Cu(II) is mainly located in the equatorial plane, and the spin density on its axial position is expected to be very small. These magnetic interactions tend mainly to be slightly ferromagnetic, although in some cases the coupling can also be slightly antiferromagnetic. The absolute J value mainly depends on the axial Cu−O distances: if this length is ca. 2.3−2.4 Å (the most frequent cases), J lies between 8 and 0.5 cm^{-1} (ferromagnetically coupled systems)[36] and ca. −0.5 to −1 cm^{-1} (antiferromagnetically coupled systems).[37] In complex **4** the central Cu_2O_2 core is equatorial−axial coordinated with the typical axial Cu−O length (2.31 Å). Thus, the ferromagnetic coupling is comparable to the values reported in the literature for similar axial lengths.[11m] Furthermore, the Addison parameter[10] τ is 0.14 for both copper ions, indicating that there is not negligible spin density on the apical position.

Complex 5. The magnetic properties of complex **5** are shown in Figure 15 in the form of $\chi_M T$ vs T. At room

temperature $\chi_M T$ is equal to 0.85 cm^3 mol^{-1} K, the expected value for two magnetically isolated spin doublets ($g = 2.12$), and remains practically constant down to about 90 K; below that temperature this value slowly decreases to 0.80 cm^3 mol^{-1} K at 10 K and then rapidly decreases further to 0.60 cm^3 mol^{-1} K at 2 K. This behavior is typical of a very weak antiferromagnetic coupling between the two copper(II) ions.

As **5** is a dinuclear copper complex, the susceptibility data were analyzed using the Bleaney−Bowers expression[33] for two magnetically interacting local spin doublets derived from the Hamiltonian $H = -J S_1 \cdot S_2$. Least-squares best-fit results are $J = -1.61$ cm^{-1}, $g = 2.12$, and $R = 3.1 \times 10^{-6}$. Furthermore, the exact value of J can be calculated with greater accuracy through a full diagonalization of the magnetization data at 2 K.[38] The plot of the reduced magnetization data is shown in Figure 15, inset. When the field reaches 50 kG (5 T), the saturation value tends toward 2 $N\beta$. The best fit values are $J = -1.61$ cm^{-1}, $g = 2.08$, and $R = 1.3 \times 10^{-6}$. These values agree perfectly with those obtained from the susceptibility data.

The small J value is explained by the bridge that links the two copper ions: O−C−C−C−O. This magnetic coupling through two oxygen atoms from the two different carboxylates implies weak AF coupling, due to the long distance created by the three carbon atoms.

Complex 6. The magnetic properties (susceptibility and magnetization) of complex **6** are the typical ones for a mononuclear copper(II) ion following the Curie law. At room temperature $\chi_M T$ is equal to 0.442 cm^3 mol^{-1} K, the expected value for one magnetically isolated spin doublet ($g = 2.17$), and remains practically constant across the whole temperature range. Only close to 2 K do the $\chi_M T$ values become slightly smaller. The plot of the reduced magnetization data follows perfectly the Brillouin law.

Comparison with Malonate and Phenylmalonate Derivatives. Table 8 shows the main structural and magnetic data for malonate and phenylmalonate derivatives compared to those for complexes reported in this study. The corresponding references are also given in this table.

(33) Bleaney, B.; Bowers, K. D. *Proc. R. Soc. London, Ser. A* **1952**, *214*, 451.
(34) Kahn, O. *Molecular Magnetism*; VCH Publishers: New York, 1993.
(35) Chandramouli, C. V. R.; Kundu T. K.; Manoharan, P. T. *Aust. J. Chem.* **2003**, *56*, 1239 and references therein.
(36) (a) Van Albada, G. A.; Mutinaiken, I.; Roubeau, O.; Turpeinen U.; Reejijk, J. *Inorg. Chim. Acta* **2002**, *331*, 208. (b) Sain, S.; Maji, T. K.; Mostafa, G.; Lu, T.-H.; Ribas, J.; Tercero J.; Chaudhuri, N. R. *Polyhedron* **2003**, *22*, 625 and references therein.
(37) Costes, J. P.; Dahan F.; Laurent, J. P. *Inorg. Chem.* **1985**, *24*, 1018.
(38) The program for doing the full-diagonalization method was gratefully supplied by Prof. Vassilis Tangoulis, from Patras University (Greece).

Table 8. Comparison of Structural and Magnetic Data for Complexes **1**−**6** with Malonate and Phenylmalonate Analogous[a]

compd	malonate				phenylmalonate				cyclobutanedicarboxylate[b]		
	struct	bridge	J/cm^{-1}	ref	struct	bridge	J/cm^{-1}	ref	struct	bridge	J/cm^{-1}
Cu^{II} salt	1D	*syn-anti* (e-e)[c] (e-a) $\tau = 0.28$	+3.0 +1.9	28d	2D	*syn-anti* (e-e) + μ_2-oxo	+4.4	9a	2D	*syn-anti* (e-e) $\beta = 82.3$ + OCCCO (e-e)	+4.76
	[mono + dinucl + trinucl][d]	*syn-anti* (e-a) *syn-anti* (e-a) τ not given	+1.8 +1.2								
+4,4′-bipy	2D	*syn-anti* (e-e) $\beta = 72.7$	+12.4	28f, 43	2D	*syn-anti* (e-a) $\tau = 0.13$	−0.59	9c	2D	*syn-anti* (e-a) $\tau = 0.1$	−0.94
+bpe	3D	*syn-anti* (e-e) $\beta = 81.4$ *syn-anti* (e-a(O_h)) μ_2-oxo (e-a) *syn-anti* (e-e) OCCCO (e-e)	+23 +6.5 −1.0 +22	44a 44b					2D	*syn-anti* (e-a) $\tau = 0.1$	−0.67
+bpy (or 5,5-Me$_2$bpy)	1D	*syn-anti* (e-e) $\beta = 74.4$	+4.6	28e	mono dinucl	 *syn-anti* (e-a) $\tau = 0.03$		8 9b	dinucl with oxo bridges	μ_2-oxo (e-a)	+4.44
+terpy									dinucl	OCCCO (e-e)	−1.61
+phen	mono- π−π stack			42	1D	*syn-anti* (e-a) $\tau = 0.10$	+0.31	8	dinucl mono- π−π stack		

^{a} β (torsion or dihedral angle between the two copper basal planes for equatorial−equatorial conformation; τ = Addison parameter,[10] for equatorial−axial conformation). ^{b} This work. ^{c} e = equatorial; a = axial. ^{d} The complex contains mononuclear, dinuclear, and trinuclear entities.

The structures of the simple copper malonate and copper phenylmalonate are rather different from the structure of complex **1**, indicating that the presence of substituents on the malonate array is not innocent from a structural viewpoint. In all of them the magnetic pathway is due to a *syn-anti* carboxylate bridge. The copper malonate has three different structures with different carboxylate binding modes. Furthermore, two other similar copper−malonate complexes have also been reported but without magnetic studies.[39] The copper phenylmalonate has a 2D structure with a *syn-anti* carboxylate coordination mode, in equatorial−equatorial fashion. Complex **1** has a 2D structure but different from that of phenylmalonate (see Table 8).

The copper malonate with 4,4′-bipy has a 2D structure formed by square grids, linked to one another by the 4,4-bipy ligand. The bridging carboxylate exhibits the *syn-anti* coordination mode in equatorial−equatorial fashion. Complex **2**, in contrast, has a different 2D structure (see structural section) with a *syn-anti* coordination mode but in equatorial−axial fashion, similar to that for the phenylmalonate analogue.

The copper malonate with the bpe ligand has a 3D structure made up of neutral corrugated malonate-bridged copper(II) layers linked through bis-monodentate bpe ligands. The bridging carboxylate exhibits the *syn-anti* coordination mode in equatorial−equatorial and equatorial−axial alternating modes. However, the presence of a double μ-oxo bridge linking equatorial−axial positions can affect the magnitude of the calculated J values. Complex **3**, in contrast, has a 2D structure (see structural section) with a *syn-anti* coordination mode but only in equatorial−axial fashion.

The copper malonate with the bpy ligand presents a 1D structure made up of malonate-bridged zigzag copper(II) chains grouped in an isosceles triangle. The coupling is through the *syn-anti* (equatorial−equatorial) carboxylate bridges. Furthermore, two mononuclear [Cu(mal)(bpy)] complexes have also been reported.[40,45] On the contrary, complex **4** has a discrete dinuclear structure (see structural section) but with two μ-oxo bridging ligands in apical−equatorial coordination mode.

The versatility of this system formed by Cu^{2+}, malonate, and bpy or derivatives can be illustrated by considering the structure of three derivatives with 4,4′-dimethyl-2,2′-bpy[41] and 5,5′-dimethyl-2,2′-bpy.[9b] All three complexes are mononuclear. With phenylmalonate the complex with bpy is mononuclear[8] and with 5,5′-dimethyl-2,2′-bpy is a dinuclear system,[9b] bridged by the carboxylate in an apical−equatorial *syn-anti* coordination mode. No magnetic data are reported.

With terpy as a blocking ligand, only complex **5** has been reported (this study). The magnetic pathway is the

(39) (a) Chattopadhyay, D.; Chattopadhyay, S. K.; Lowe, P. R.; Schwalbe, C. H.; Mazumber, S. K.; Rana, A.; Ghosh, S. *J. Chem. Soc., Dalton Trans.* **1993**, 913. (b) Yilmaz, V. T.; Senel, E.; Thöne, C. *Transition Met. Chem.* **2004**, *29*, 336.

(40) Suresh, E.; Bhadbhade, M. *Acta Crystallogr.* **1997**, *C53*, 193.

(41) Gasque, L.; Moreno-Esparza, R.; Molins, E.; Briansó-Peñalva, J. L.; Ruiz-Ramírez, L.; Medina-Dickinson, G. *Acta Crystallogr.* **1998**, *C54*, 1848.

(42) Gasque, L.; Moreno-Esparza, R.; Molins, E.; Briansó-Peñalva, J. L.; Ruiz-Ramírez, L.; Medina-Dickinson, G. *Acta Crystallogr.* **1999**, *C55*, 158.

(43) (a) Li, J.; Zeng, H.; Chen, J.; Wang, Q.; Wu, X. *Chem. Commun.* **1997**, 1213. (b) Li, J.-M.; Zhang, Y.-G.; Chen, J.-H.; Rui, L.; Wang, Q.-M.; Wu, X.-T. *Polyhedron* **2000**, *19*, 1117.

(44) (a) Delgado, F. S.; Sanchiz, J.; Ruiz-Pérez, C.; Lloret, F.; Julve, M. *Inorg. Chem.* **2003**, *42*, 5938. (b) Sain, S.; Maji, T. K.; Mostafa, G.; Lu, T.-H.; Chaudhuri, N. R. *New J. Chem.* **2003**, *27*, 185.

(45) Shen, H.-Y.; Bu, W.-M.; Liao, D.-Z.; Jiang, Z.-H.; Yan, S.-P.; Wang, G.-L. *Inorg. Chem. Commun.* **2000**, *3*, 497.

(46) (a) Liu, T.-F.; Sun, H.-L.; Gao, S.;.Zhang, S.-W; Lau, T.-C. *Inorg. Chem.* **2003**, *42*, 4792. (b) Zhang, X.; Lu, C.; Zhang, Q.; Lu, S.; Yang, W.; Liu, J.; Zhuang, H. *Eur. J. Inorg. Chem.* **2003**, 1181.

(47) Sanchis, J.; Rodríguez-Martín, Y.; Ruiz-Pérez, C.; Mederos, A.; Lloret, F.; Julve, M. *New J. Chem.* **2002**, *26*, 1624.

−OCCCO− group of the cbdca, thus giving small anti-ferromagnetic coupling (see Table 8).

With phen, the malonate derivative and complex **6** have a similar structure: a discrete mononuclear one with strong $\pi-\pi$ interactions. With 5,6-dimethyl-1,10-phenanthroline and malonate a mononuclear structure is also formed.[42] However, with phenylmalonate the structure corresponds to a one-dimensional complex.

Conclusions

Six new compounds were prepared, and their structures and magnetic properties were investigated. In these complexes the cbdca ligand acts as a bridging (**1**−**5**) or as a blocking ligand (**6**); in the latter compound the weak interactions (hydrogen bonding and $\pi-\pi$ stacking) govern the structure, giving rise to a two-dimensional network. Compounds **1**−**3** are all two-dimensional polymers, but their structures are different. There are two bridging ligands in compounds **2** and **3** (cbdca and bipy or bpe, respectively) and only one in **1** (cbda). Compounds **4** and **5** are neutral dinuclear Cu(II) cations, but their structures are very different. In compound **4**, two carboxyl oxygen atoms from different cbdca ligands act as a μ_2-oxo bridge, whereas, in compound **5**, one oxygen from each carboxylate group binds a different metal as unidentate and the rest of the oxygen remains uncoordinated. A comparison with the related malonate and phenylmalonate copper(II) derivatives reveals that the presence of the cyclobutane ring on the methylene carbon exerts important structural effects.

From a magnetic point of view, all compounds display weak interactions, caused mainly by either the *syn-anti* conformation of the carboxylate bridge or by the long bridge distance in compound **5**. From these new complexes it is possible to corroborate the findings about the magnetic coupling derived from *syn-anti* carboxylate bridging ligands: when the conformation is equatorial−equatorial, J changes gradually from AF to F when the copper planes changes from parallel to perpendicular between them. On the contrary, when the conformation is equatorial−axial, the magnetic coupling is always very small, but it can be F or AF depending on subtle structural changes, impossible to define to date.